MIPS: Multiphase Integrated Planar Symmetric Coupled Inductor for Ultra-Thin VRM

Jaeil Baek, *Member, IEEE*, Youssef Elasser, *Student Member, IEEE*, and Minjie Chen, *Senior Member, IEEE*

***Abstract*—Multiphase coupled inductor is a key technology for ripple reduction and fast transient in pulse-width-modulated power converters. This letter presents the modeling and design of Multiphase Integrated Planar Symmetric (MIPS) coupled inductor, together with a hybrid-switched-capacitor dc-dc converter for ultra-thin multiphase point-of-load voltage regulation modules. The benefits of MIPS inductors are quantified. A systematic approach to designing high performance multiphase MIPS inductors is introduced and validated by a 10 V input, 1 V output, 10 A 2-level four-phase coupled 3 MHz hybrid-switched-capacitor dc-dc converter with compact size and fast transient.**

***Index Terms*—coupled inductor, hybrid-switched-capacitor dc-dc converter, thin-flat core, voltage regulation module**

I. Introduction

The rapidly increasing power demand of future high performance microprocessors makes vertical power delivery extremely attractive [1], [2]. It is critical to minimize the z-height of voltage regulation modules (VRMs) to enable ultra-compact power systems in packaging (PwrPACK) and reduce the interconnect lengths (Fig. 1). As shown in Fig. 2, discrete inductors usually set the z-height of VRMs. The miniaturization of the inductors is limited by the fundamental trade-off between transient and ripple performance of the VRM. One method of addressing this trade-off is to replace the discrete inductors in interleaved multiphase PWM topologies with coupled inductors [3], [4]. Coupled inductors can enable both high di/dt in transient and low current ripple in steady state with much reduced dc energy storage and magnetic size. Various coupled inductor structures have been proposed, including vertical structure [2], planar structure [3], [5], matrix structure [4], and PCB-embedded winding structures [6].

Figure 3 shows a few multiphase integrated planar symmetric (MIPS) coupled inductors ranging from two-phase to M-phase. Similar two-phase coupled and multiphase weakly coupled inductors have been explored in [7], [8]. However, structures and models for multiphase strongly coupled inductors have not been thoroughly investigated. We present a systematic approach to designing multiphase strongly coupled inductors with low z-height. The MIPS inductor has multiple symmetrically placed vias. Each via contains two windings with reverse currents to eliminate the dc flux and reduce the ripple. Each winding goes through two neighboring vias. The magnetomotive force (MMF) of all windings points toward the same direction (inside or outside). One can adjust the via placements to adjust the coupling coefficients. The MIPS inductor is then attached to a printed circuit board (PCB) or a silicon substrate. Compared to the previous weakly coupled inductors [7], [8], the MIPS coupled inductor offers (1) fully symmetric multiphase coupling; (2) simpler lumped circuit model and straightforward optimization method; (3) significant current ripple reduction due to high coupling coefficient; (4) easy manufacturing, and (5) mechanical robustness.

The MIPS coupled inductor leverages coupling and interleaving for improved performance, and offers ultra low z-height. It has the potential to be fabricated on-chip or in packaging. A 3 MHz 10 V input, 1 V/10 A output two-level series-capacitor buck converter with a four-phase 2.1 mm height core was built and tested. We introduce the modeling and design of the MIPS inductor, optimize the hybrid-switched-capacitor dc-dc converter, and present experimental results to verify the

This work was supported by Semiconductor Research Corporation (SRC). (Corresponding author: Minjie Chen.) The authors are with the Department of Electrical and Computer Engineering and Andlinger Center for Energy and the Environment at Princeton University, Princeton, NJ 08540, USA.

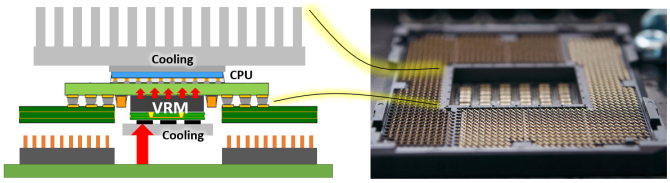

Fig. 1. Vertical power delivery to high current microprocessors with an ultra-thin voltage regulation module embedded in packaging.

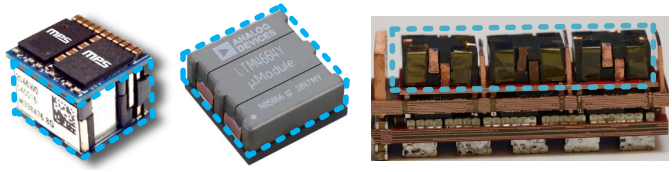

Fig. 2. State-of-the-art voltage regulations modules with magnetics dominating the system z-height (MPS PC22161, ADI TM4664, LEGO-PoL [2]).

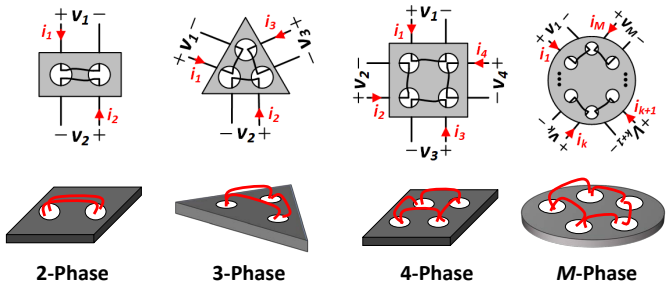

Fig. 3. Principle and conceptual drawings of a few example MIPS inductors. Different from the lateral flux inductors presented in [7], [8] where each magnetic via has a single winding, each magnetic via in the MIPS inductor contains two windings with interleaved current flow in reverse directions.

effectiveness of the key principles.

II. Modeling and Design of MIPS Inductors

Figure 4 labels the dimension and design parameters of a four-phase MIPS coupled inductor core. The thin-plate magnetic core contains four evenly spaced vias. Each via contains two windings. Each winding creates a lateral flux pointing toward the center of the core. Figure 5 presents the modeling and design procedure for a M phase symmetric design with the core plate considered as circular plate with a radius of R. The windings in a MIPS inductor can have multiple turns. They can be modeled as multiple $N:1$ ideal transformer as illustrated in the inductance dual model in Fig. 5. The vias are placed at a radius of h. $\mathcal{R}_s$ and $\mathcal{R}_l$ represent the reluctance of each lumped segment of the core, and $\mathcal{R}_a$ represents the leakage flux path through the air. $\mathcal{R}_s$ and $\mathcal{R}_l$ are determined by h and z. For a given R, as h increases, $\mathcal{R}_s$ reduces and $\mathcal{R}_l$ increases. As z increases, both $\mathcal{R}_s$ and $\mathcal{R}_l$ reduce. The reluctance model is then converted into an inductance dual model with inductance values equal to $1/\mathcal{R}_s$, $1/\mathcal{R}_l$ and $1/\mathcal{R}_a$, respectively.

1) If $\mathcal{R}_l$ is comparable or smaller than $\mathcal{R}_s$ (small d), the multiple windings are well coupled. The inductance dual model simplifies into a standard symmetric model as described in [3] with leakage inductance equal to $M/\mathcal{R}_a$, and magnetizing inductance equal to $1/(\mathcal{R}_s + \frac{M-1}{2M}\mathcal{R}_l)$. With duty ratio D and phase number M, define an integer index k such that $\frac{k}{M} \le D \le \frac{k+1}{M}$, the phase current ripple of an interleaved multiphase buck converter with coupled inductor ($\Delta i_{phase}^{coupled}$) is reduced compared to that with uncoupled inductors ($\Delta i_{phase}^{non-coupled}$) with the same transient response is described by a factor γ:

$$\gamma \overset{\text{def}}{=} \frac{\Delta i_{phase}^{coupled}}{\Delta i_{phase}^{non-coupled}} = \frac{1+\beta\Gamma}{1+\beta}. \quad (1)$$

Here $\beta = \mathcal{R}_a/(\mathcal{R}_s + \frac{M-1}{2M}\mathcal{R}_l)$ is the ratio between the reluctance of the leakage path and the magnetizing path. A higher β indicates stronger coupling. Γ is the ripple reduction ratio of multiphase interleaving $\Gamma = \frac{(k+1-DM)(DM-k)}{(1-D)DM^2}$. Figure 6 plots γ as a function of β, D, and M. γ reduces as M and β increase, and reaches the minimum when D is equal to k/M.

2) If $\mathcal{R}_l$ is much larger than $\mathcal{R}_s$, the multiple windings are decoupled. Each winding functions as a discrete inductor with its inductance value equals $1/(\mathcal{R}_s + \mathcal{R}_a)$.

For a four-phase symmetric design based on a square core with $x = y$, $\mathcal{R}_s$ can be estimated as $\frac{1}{\mu}\frac{(x+d)/2}{dz}$, and $\mathcal{R}_l$ can be estimated as $\frac{1}{\mu}\frac{(x+d)/2}{z(x-d)/2}$. β reaches the maximum when $\mathcal{R}_s + \frac{M-1}{2M}\mathcal{R}_l$ is at the minimum when $d/x = \sqrt{6}-2 = 0.45$. This is the optimal d/x that maximizes the β. However, a maximum β does not indicate the smallest absolute phase current ripple. d/x can be further increased to reduce the ripple (by reducing the $\mathcal{R}_s$ and increasing the magnetizing inductance), at the cost of reduced transient response (di/dt).

The optimal d/x ratio can be found more precisely with finite-element-analysis (FEA). Figure 7 shows the ANSYS

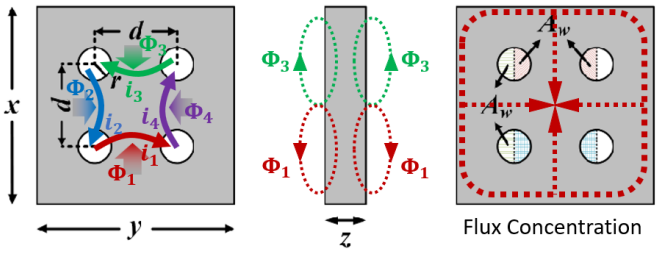

Fig. 4. Design parameters for a four-phase MIPS coupled inductor: x-length, y-width, z-core height, r-via radius, d-via distance, and A_w-winding area. All windings have the same number of turns and winding area.

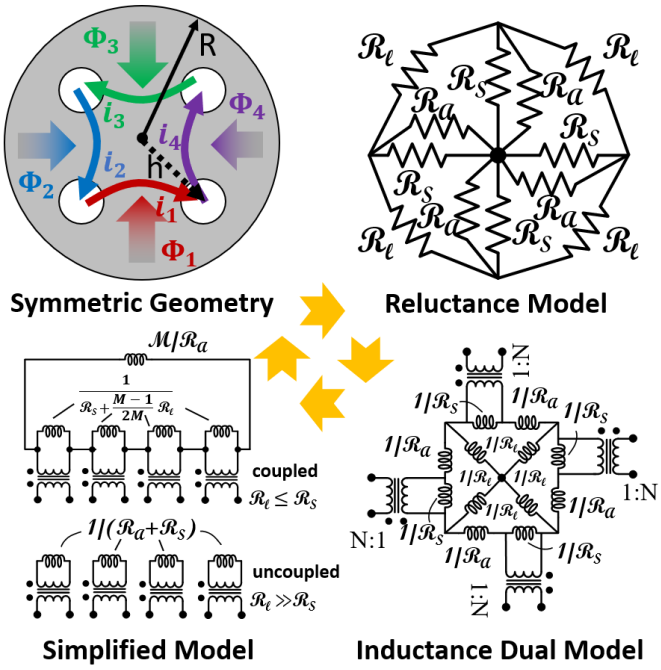

Fig. 5. Modeling and design of a four-phase MIPS coupled inductor including: (1) Physical geometry; (2) Reluctance model; (3) Inductance dual model; and (4) Simplified standard model if $\mathcal{R}_s \gg \mathcal{R}_l$ or $\mathcal{R}_s \ll \mathcal{R}_l$.

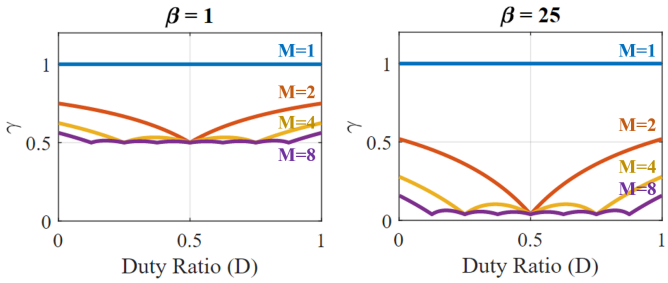

Fig. 6. Phase current ripple reduction factor (γ) for an M-phase interleaved buck converter with duty ratio D, phase number M, and coupling coefficient β. γ quantifies the benefit of interleaving and coupling for phase current ripple reduction in multiphase buck converters.

Maxwell simulation results of a four-phase MIPS coupled inductor with different d and z for a fixed 11-mm by 11-mm core. L_{pss} is the effective inductance determining the phase current ripple [3]. With a high permeability core ($\mu_r = 900$), the core height (z) has very low impact on the transient performance. z is also usually determined by design factors such as total packaging height. With fixed x, y, and z, d sets the self-inductance and coupling coefficients of the windings,

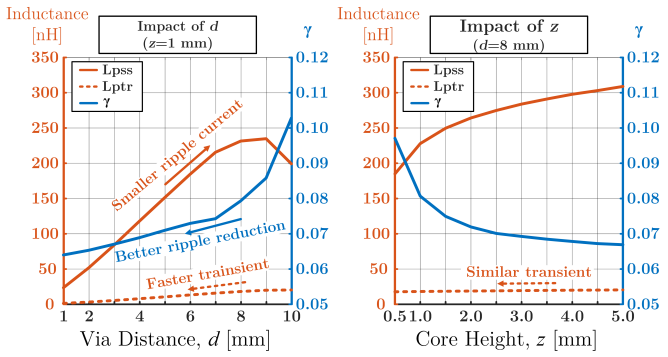

Fig. 7. Finite element simulation results of per phase steady state inductance (L_{pss}), per phase transient inductance (L_{ptr}), and ripple reduction ratio (γ) for a four-phase MIPS coupled inductor with different via distance (d) and core height (z). The via distance of the prototype core is selected as 5.5 mm.

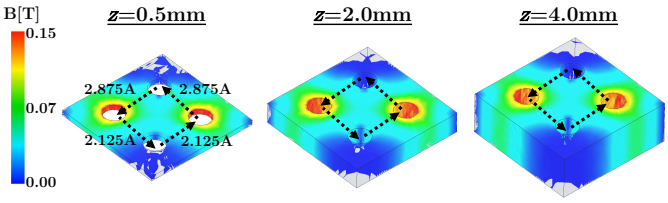

Fig. 8. Finite element modeling of three different four-phase MIPS coupled with 30% (0.75 A) phase current mismatch. The x and y of the core are 11 mm. The z heights of the cores are 0.5 mm, 2 mm and 4 mm. The simulated maximum flux density with the 2 mm z-height core is about 130 mT.

and thus determines the transient and ripple performance of the coupled inductor. As d increases, the self inductance increases (i.e., smaller current ripple), and the coupling coefficient reduces (i.e., less advantage from coupling). d and z should be jointly optimized to balance the current ripple and transient response.

Phase current imbalance can significantly impact the flux density distribution in a coupled inductor. Circuit-magnetic co-design and time-domain circuit simulations are usually needed to evaluate the worst-case scenario and avoid core saturation when phase current imbalance exists. The inductance dual model shown in Fig. 5 can be directly utilized in circuit simulations to visualize the flux distribution in each segment of the magnetic core, especially when phase current mismatch exists and if the core thickness is very thin. The current in $1/\mathcal{R}_s$ is proportional to the flux through the intersection core segment between two vias. The current in $1/\mathcal{R}_l$ is proportional to the flux flowing through the outside core segment close to the edge. The current in $1/\mathcal{R}_a$ is proportional to the leakage flux through the air. High permeability, high saturation limit magnetics fit particular well to the MIPS inductor design.

III. Experimental Results

The MIPS coupled inductor can replace the discrete inductors in various multi-phase PWM converters, series-capacitor buck converters, forward converters, and many other PWM converters. It can also replace dc-link inductors with significant dc energy storage in resonant converters, such as the choke inductors in Class-E inverters. Figure 9 shows a two-phase

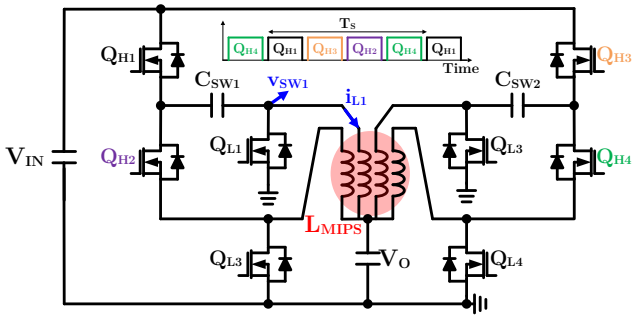

Fig. 9. 10 V to 1 V/10 A 3 MHz four-phase series-capacitor-buck converter with a four-phase MIPS inductor. Two series-capacitor-buck converters are connected in parallel with 90° phase shift to enable equal four-phase interleaving.

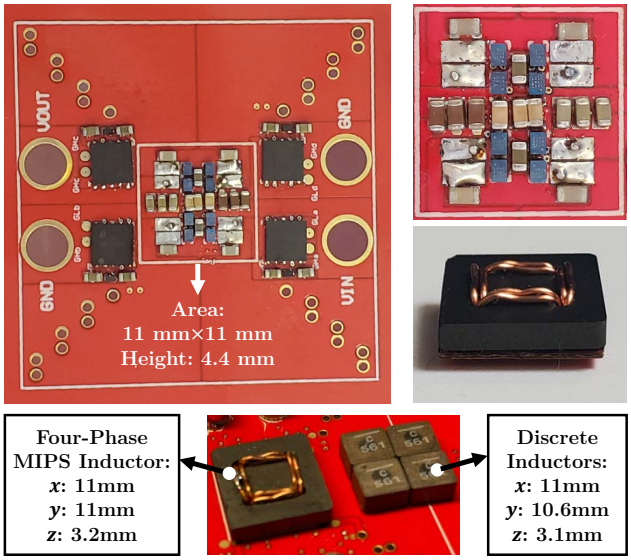

Fig. 10. Picture of the prototype with a designed four-phase MIPS coupled inductor. The dimensions of the MIPS inductor are: x=11-mm, y=11-mm, d=5.5-mm, r=1-mm, z=3.2-mm (core:2.1-mm, winding 1.1-mm). Each winding has two turns.

two-level series-capacitor buck converter with a four-phase MIPS inductor as a design example. The two-levels within one series-capacitor module are 180° phase-shifted, and the two-phases are 90° phase-shifted. The duty ratio of this series-capacitor circuit is extended by a factor of two for the same input output voltage conversion ratio. Figure 10 shows a picture of the prototype. The power stage area is 121 mm^2 including input capacitors (10 μF X5R, 0.1 μF X7R), output capacitors (22 μF X7R, 10 μF X7R), series-capacitors (1 μF X7R), switches (EPC-2216), and a MIPS inductor wire-bonded to the other side of the power stage. The 11 mm×11 mm×3.2 mm four-phase MIPS inductor was fabricated with a Hitachi ML91S I core. The via radius is 0.8 mm. The via-to-via distance is 5.5 mm. The four windings each has two turns with 24 AWG wires. The dc resistance of each phase is 1.5 mΩ. The four-phase MIPS-inductor and four 560 nH discrete inductors (XFL5030-561) with 3.8 mΩ dc resistance (DCR) are shown. LM5113 was used for driving EPC-2216. The two inductors have similar phase inductance and current ripple. The converter switches between 2-to-3 MHz with 10

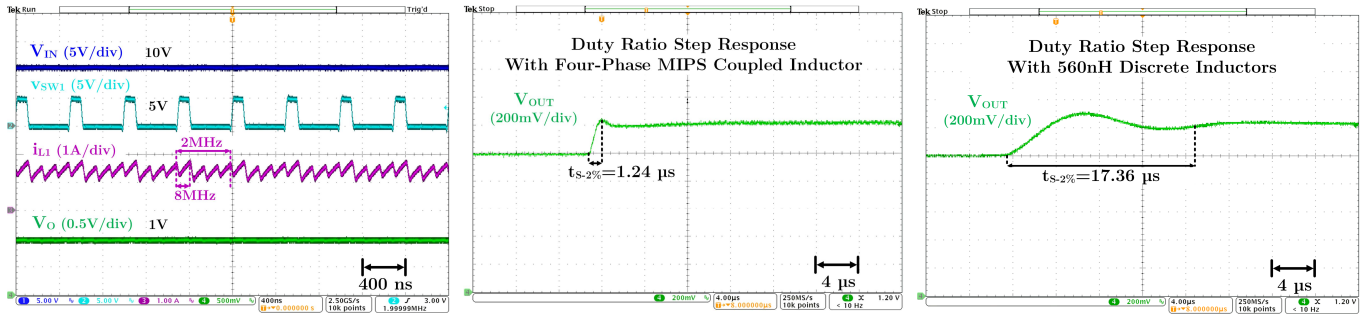

(a) (b) (c)

Fig. 11. Measured waveforms of the prototype at 10 V input and 1 V/6 A output. (a) Steady-state operation with the four-phase MIPS inductor. (b) Duty-step transient waveforms with the four-phase MIPS inductor. (c) Duty-step transient waveforms with four 560 nH discrete inductors. The four-phase MIPS inductor achieves a similar steady-state ripple current to the discrete inductor and a much faster transient response than the discrete inductor.

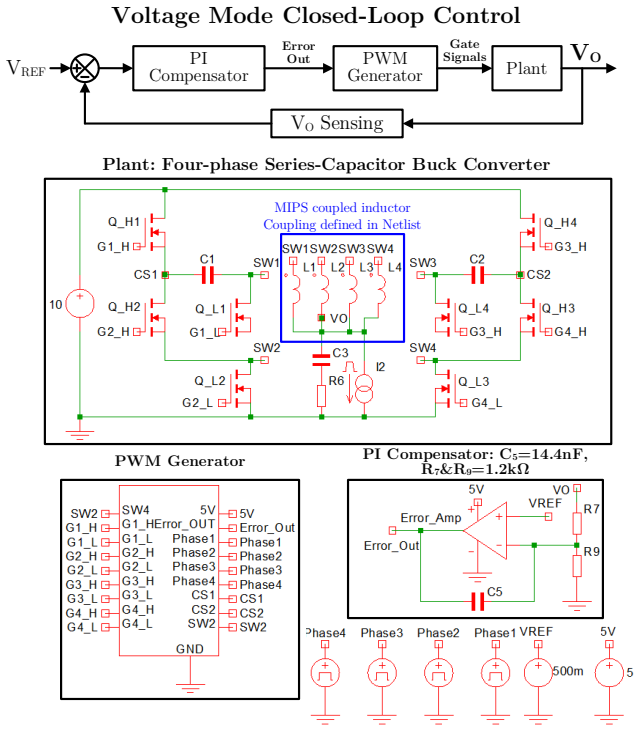

Fig. 12. SIMetrix simulation platform of the prototype four-phase series capacitor buck converter with a standard voltage mode closed-loop control.

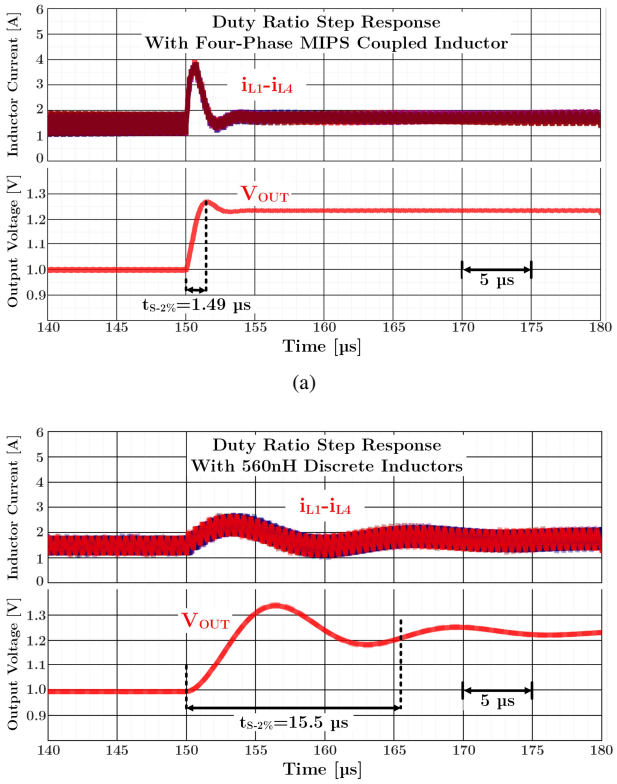

Fig. 13. Simulated open loop duty ratio step response of the series-capacitor buck converter at 10 V input and 6 A output for active voltage positioning: (a) A four-phase MIPS coupled inductor. (b) Four 560 nH discrete inductors.

V input, 1 V and 11 A output. The simulated self and leakage inductance per phase are 4.276 μH and 47 nH. The measured self and leakage inductance per phase are 4.646 μH and 40 nH, respectively. This represents a β of 121 with a γ of 7% compared to a non-coupled case with a duty ratio D of 20%. The measured 8 MHz 0.75 A phase current ripple (Fig. 11a) matches with the estimation.

A key advantage of multiphase coupled inductor is the faster transient response with the same phase current ripple. Figure 11a shows the measured waveforms with the MIPS coupled inductor. The prototype with the designed coupled inductor has a small ripple current at 8 MHz, which is similar to the 2-MHz current ripple of a 560 nH discrete inductor. The series-capacitor mechanism forces current sharing among the four-phases. The output voltage ripple is very small due to multiphase interleaving. Figures 11b and 11c show the output voltage waveforms in response to a switch duty ratio change, which reflects the step-response of the duty ratio to output voltage transfer function. The small transient inductance of the MIPS inductor (40 nH) enables the output voltage to settle within 2% of its expected value in 1.24 μs, which is much faster than the 17.36 μs when using four 560 nH discrete inductors for a comparable phase current ripple. Fig. 12 shows a SIMetrix simulation platform of the four-phase series capacitor buck converter with a voltage mode closed loop. EPC-2216 SPICE model and measured inductance matrix of the four-

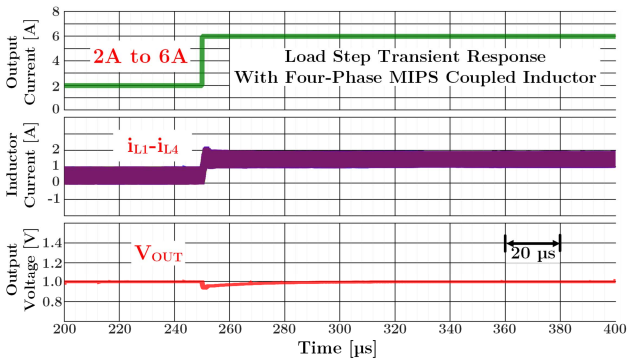

(a)

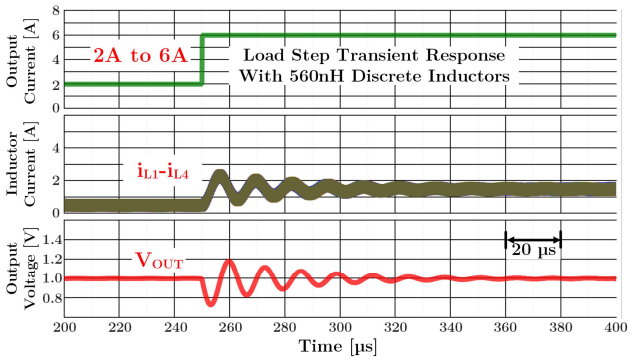

(b)

Fig. 14. Simulated closed-loop transient waveforms of series-capacitor buck converters with 2 A to 6 A (0.5 A/ns slew rate) load step at 10 V input and 1 V output for fast current regulation: (a) A four-phase MIPS coupled inductor. (b) Four 560 nH discrete inductors.

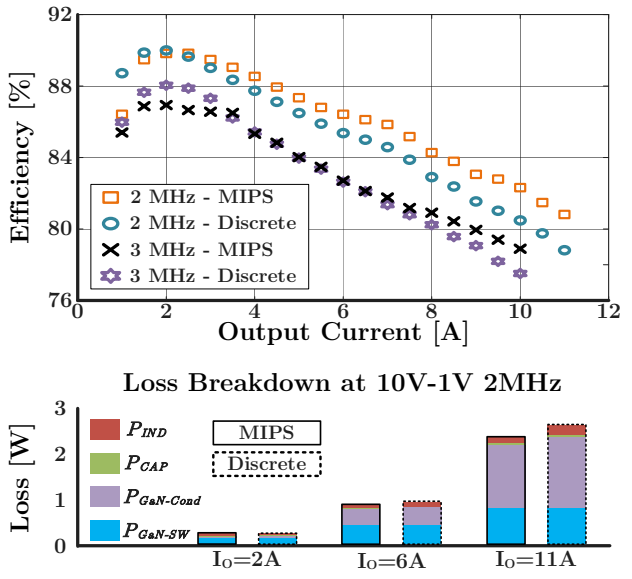

Fig. 15. Measured efficiency at 10 V input / 1 V output at the different switching frequencies and loss breakdown. The hotspot (GaN devices) temperature was kept below 100°C with natural cooling (25°C ambient air temperature).

phase MIPS inductor are included. Figures 13 and 14 show the simulated open-loop and closed-loop transient waveforms. The open-loop duty-step transient results are similar with the experimental results and current ramp-up slope of the four-phase MIPS inductor (Fig. 13a) is much faster than the 560-nH discrete inductors (Fig. 13b). The small transient inductance of the MIPS inductor enables much faster load-step response even with the same PI compensator design (Fig. 14), and allows for high control bandwidth because it can push the double poles to a higher frequency with high di/dt for current regulation.

Figure 15 shows the measured efficiency of the converter using a MIPS inductor and four discrete inductors. The designed coupled inductor enables the prototype to achieve similar light load efficiency with 560-nH inductor due to the similar phase current ripple, while achieving higher heavy load efficiency with smaller DCR (1.5-mΩ) than discrete inductors (3.8-mΩ). Due to the high core loss of ML91S at 3 MHz, the MIPS inductor results in lower efficiency at light load. The MIPS inductor can replace the discrete inductors in various multiphase converters while achieving similar efficiency and power density performance but much faster transient response.

IV. Conclusion

This letter presents the modeling and design of Multiphase Integrated Planar Symmetric (MIPS) coupled inductor. The MIPS inductor comprises a planar core and multiple vertical vias each hosting two windings with current in reverse directions. It offers better ripple reduction and transient performance than discrete inductors, and can be easily manufactured. MIPS inductor can replace the discrete inductors in many PWM or resonant power converters to reduce the $\frac{1}{2}LI_{dc}^2$ energy storage. A 3-MHz 10 V input, 1 V/10 A output two-phase-interleaved two-level series-capacitor buck converter was built and tested to verify the principles of the MIPS inductor. The MIPS inductor fits particularly well to multiphase interleaved voltage regulation modules (VRMs) when low-profile inductor, small ripple, high-efficiency, and fast transient response are needed.

References

[1] F. C. Lee and Q. Li, "High-Frequency Integrated Point-of-Load Converters: Overview," *IEEE Trans. on Power Electron.*, vol. 28, no. 9, pp. 4127-4136, Sept. 2013.

[2] J. Baek et al., "Vertical Stacked LEGO-PoL CPU Voltage Regulator," *IEEE Trans. on Power Electron.*, vol.37, no.6, pp. 6305-6322, Jun. 2022.

[3] M. Chen and C. R. Sullivan, "Unified Models for Coupled Inductors Applied to Multiphase PWM Converters," *IEEE Trans. on Power Electron.*, vol. 36, no. 12, pp. 14155-14174, Dec. 2021.

[4] P. Wang, D. Zhou, Y. Elasser, J. Baek, and M. Chen, "Matrix Coupled All-in-One Magnetics for PWM Power Conversion," *IEEE Trans. on Power Electronics*, vol. 37, no. 12, Dec. 2022.

[5] A. Stratakos, C. R. Sullivan and J. Li, "Method for making magnetic components with N-phase coupling, and related inductor structures," U.S. Patent 8,350,658, January 8, 2013.

[6] M. Ursino et al., "High density 48V-to-PoL VRM with hybrid pre-regulator and fixed-ratio buck," *IEEE Applied Power Electronics Conference and Exposition (APEC)*, 2020, pp. 498-505.

[7] Q. Li, Y. Dong, F. C. Lee and D. J. Gilham, "High-Density Low-Profile Coupled Inductor Design for Integrated Point-of-Load Converters," *IEEE Transactions on Power Electronics*, vol. 28, no. 1, pp. 547-554, January 2013.

[8] D. Hou, F. C. Lee and Q. Li, "Very High Frequency IVR for Small Portable Electronics With High-Current Multiphase 3-D Integrated Magnetics," *IEEE Transactions on Power Electronics*, vol. 32, no. 11, pp. 8705-8717, Nov. 2017.